Atmos. Chem. Phys. Discuss., 13, 14613–14635, 2013
www.atmos-chem-phys-discuss.net/13/14613/2013/
doi:10.5194/acpd-13-14613-2013

Atmospheric Chemistry and Physics Discussions

The role of low volatile organics on secondary organic aerosol formation

H. Kokkola[1], P. Yli-Pirilä[2], M. Vesterinen[1], H. Korhonen[1], H. Keskinen[2], S. Romakkaniemi[2], L. Hao[2], A. Kortelainen[2], J. Joutsensaari[2], D. R. Worsnop[3,2], A. Virtanen[2], and K. E. J. Lehtinen[1,2]

[1]Finnish Meteorological Institute, Kuopio Unit, P.O. Box 1627, 70211, Kuopio, Finland
[2]University of Eastern Finland, P.O. Box 1627, 70211, Kuopio, Finland
[3]Aerodyne Research Inc., Billerica, MA, 01821-3976, USA

Received: 16 May 2013 – Accepted: 21 May 2013 – Published: 4 June 2013

Correspondence to: H. Kokkola (harri.kokkola@fmi.fi)

Published by Copernicus Publications on behalf of the European Geosciences Union.

Abstract

Large-scale atmospheric models, which typically describe secondary organic aerosol (SOA) formation based on chamber experiments, tend to systematically underestimate observed organic aerosol burdens. Since SOA constitutes a significant fraction of atmospheric aerosol, this discrepancy translates to an underestimation of SOA contribution to climate. Here we show that the underestimation of SOA yields can partly be explained by wall-losses of SOA forming compounds during chamber experiments. We present a chamber experiment where α-pinene and ozone are injected in a Teflon chamber. When these two compounds react, we observe rapid formation and growth of new particles. Theoretical analysis of this formation and growth event indicates rapid formation of oxidized organic compounds (OVOC) of very low volatility in the chamber. Although these OVOCs of very low volatility contribute to the growth of new particles, their mass will almost completely be depleted to the chamber walls during the experiment while the depletion of OVOCs of higher volatilities is less efficient. According to our model simulations, the volatilities of OVOC contributing to the new particle formation event are of the order of 10^{-5} µg m^{-3}.

1 Introduction

Organic chemical compounds modify the physical and chemical properties of atmospheric aerosol particles; the radiative properties, their ability to act as cloud condensation nuclei, and the heterogeneous chemistry. Organic compounds (OC) amount to a significant fraction in atmospheric aerosol mass. In several observations at different types of locations, the measured mass fraction of organic compounds can be 20–90 % in collected aerosol samples (Jimenez et al., 2009). Thus, OC is in a major role in the climate effects of global atmospheric aerosol.

Organic aerosol can be emitted directly into the atmosphere as primary particles, e.g. from fossil fuel and biomass combustion, or they can be of secondary origin; when

ACPD
13, 14613–14635, 2013

volatile organic compounds (VOC) are oxidized in the atmosphere they produce oxidized organic compounds (OVOC) which condense on pre-existing aerosol forming secondary organic aerosol (SOA). As the SOA compounds are in a major role in the atmospheric aerosol processes, their contribution in the global aerosol mass and composition are in a key role when predicting their effects on climate using atmospheric models. However, current global aerosol–climate models in which the SOA description is based on oxidation chamber experiments (bottom-up approach) tend to underestimate the fraction of SOA in the global aerosol mass when compared to observations or to approaches where global SOA burdens are determined inversely based on VOC emission data and estimates of SOA removal (top-down approach) (Jimenez et al., 2009; Goldstein and Galbally, 2007; Hallquist et al., 2009). This underestimation that can be more than one order of magnitude and may lead to significant errors when predicting global aerosol forcing (Goldstein and Galbally, 2007; Hallquist et al., 2009).

The difficulty in properly modeling SOA formation is that the chemical composition and formation pathways of condensing organic compounds that take part in SOA formation are still very much unknown and their volatility undergoes continuous change in the atmosphere for several days (Kroll and Seinfeld, 2008). Information on volatility of ambient organic compounds would be of crucial importance when SOA formation is estimated as the OVOC's of low volatility (LVOC) have an important role when the freshly formed particles grow to sizes that can form cloud droplets (Riipinen et al., 2011). In addition, a recent study has shown that oxidized organics can also be involved in aerosol nucleation process (Zhao et al., 2013). This so far, it has been speculated that the formation of LVOC's is a process that takes several hours in the atmosphere (Jimenez et al., 2009).

The extremely large number of chemical compounds involved in SOA formation processes makes it a challenging task to calculate the concentration of a specific oxidation product. Even explicit chemistry models have great uncertainties in predicting the oxidation state of ambient SOA precursors (Ceulemans et al., 2012). Furthermore, they are computationally too demanding to be coupled to models that describe SOA con-

ACPD
13, 14613–14635, 2013

centrations in regional or global scale. To overcome this complexity, simplified methods have been developed to describe OVOC's that are involved in the formation of SOA. A common way is to categorize different organic compounds according to their volatility, i.e. the saturation vapor pressure. Two commonly used methods are treating SOA precursors as two model compounds of different volatilies (Odum et al., 1996) or separating the precursors into several classes according to their volatilities, namely the Volatility Basis Set (VBS) (Donahue et al., 2006).

The mass yields of SOA forming compounds from gas phase transformation of VOC are often based on chamber measurements: the yields are obtained by analyzing the observed increase in condensed particulate mass when known amount of VOC's are oxidized in a chamber (Donahue et al., 2006; Pathak et al., 2007; Meyer et al., 2009; Duplissy et al., 2011). To get information on the yields of individual volatility classes, data from aerosol particle sizers, aerosol mass spectrometers, and thermodenuders are combined to analyze the oxidation state and the volatilities of condensed compounds.

One complication in these experiments is the loss of aerosol on the chamber wall surfaces during an experiment. The measured particulate mass is affected by losses of particles to the chamber walls and the mass yields have to be corrected accordingly (Pathak et al., 2007). Recently, it has also been acknowledged that the wall losses of the gas phase compounds, i.e. SOA precursors, can have a significant effect on the SOA yields and have to be accounted for when the SOA yields are estimated (Pathak et al., 2007; Pierce et al., 2008; Matsunaga and Ziemann, 2010).

Matsunaga and Ziemann (2010) showed that for gaseous organic compounds there is an equilibrium between the walls and the gas phase, unlike for the aerosol particles for which the walls act as a sink. They suggested a method to calculate the partitioning between the walls and the gas phase as equilibrium similarly as when assuming Henry's law equilibrium. According to their theoretical framework, the fractions of dif-

ACPD
13, 14613–14635, 2013

ferent OC partitioned on the walls were determined by the equation:

$$\frac{[\mathrm{OC}]_\mathrm{w}}{[\mathrm{OC}]_\mathrm{T}} = \frac{K_\mathrm{p}}{(K_\mathrm{p}+1)}, \quad (1)$$

where $[\mathrm{OC}]_\mathrm{w}$ is the number of moles of OC on the wall, $[\mathrm{OC}]_\mathrm{T}$ is the total number of moles of OC in the chamber, and K_p is the partitioning coefficient. The partitioning coefficient K_p was calculated according to

$$K_\mathrm{p} = K_\mathrm{w} C_\mathrm{w} = \frac{RTC_\mathrm{w}}{M_\mathrm{w}\gamma_\mathrm{w}P^\circ} \quad (2)$$

where K_w is the gas–wall partition coefficient, C_w is the effective concentration of OC on the chamber wall, R is the gas constant, T is temperature, M_w is the molar mass of OC, γ_w is the OC activity coefficient for the Teflon wall (assumed 1 in our simulations), and P° is the saturation vapor pressure of OC.

Such an equilibrium state would have significant consequences on SOA formation as the OVOC's would strive to reach simultaneous equilibrium among the particles, the gas phase, and the walls (see Fig. 1). For example, if the condensation of OVOC's to the particles depletes them from the gas phase, OVOC's already deposited on the chamber walls will evaporate to maintain the wall–gas equilibrium. This makes it more complex to account for the wall losses of OVOC's during a chamber experiment compared to an approach where gas deposition to the wall is considered irreversible. Another difficulty related to this method is that the equilibrium is dependent on the wall partitioning properties of each chemical compound. If this approach is used to account for the wall losses for all oxidation products of VOC's, the wall-partitioning properties in Eq. (1) should be quantified for each individual compound. In addition, to apply this method together with volatility basis set, the wall partitioning properties of each volatility class should be somehow defined. To illustrate SOA formation in a chamber experiments, Fig. 1 shows a schematic of all involved processes. The schematic represents an experiment, where VOC and an oxidant are injected in a chamber with pre-existing seed aerosol.

ACPD
13, 14613–14635, 2013

Here we study the implications of equilibrium wall–gas partitioning on estimated SOA yields when compounds of several different volatilities are present in a Teflon chamber. We use high resolution proton transfer reaction mass spectrometry (PTR-TOF) to estimate the gas–wall partitioning of SOA precursors as a function of saturation vapor pressure, and then formulate a generalized function for oxidation products of α-pinene. We apply this partitioning function to an aerosol microphysics model and compare model results against chamber measurements of aerosol formation and growth to estimate the implications of volatility based wall loss function on the evolution of aerosol size distribution.

2 Materials and methods

2.1 Gas–wall equilibrium partitioning

Gas–wall partitioning of organic gases (OC) was quantified by injecting three organic gases of different volatilities in a Teflon chamber and measuring the gas phase concentration after injection. The chamber setup has been described in detail by Hao et al. (2011). Briefly, the system consists of precursor and seed particle injection systems, a reaction chamber (made of FEP film, volume 4 m^3), and gas and particle measurements systems. The injected OC were pinanediol, nopinone and α-pinene whose saturation vapor pressures are 0.533 Pa, 53.6 Pa and 465.15 Pa, respectively (www.chemspider.com). Nopinone and pinanediol were chosen for this study since they are probable oxidation products of α-pinene. Experiments were performed in the absence of seed particles at a relative humidity below 5 %. The chamber was kept at constant room temperature (20 ± 1 °C) during the experiment. Before each experiment the chamber was flushed continuously with purified dry air for about 48 h to ensure minimal contamination from previous experiments. A known amount of α-pinene (Sigma-Aldrich, 99 %), nopinone (Sigma-Aldrich, 98 %) and pinanediol (Sigma-Aldrich, 99 %) were first dissolved in methanol (Fisher Chemicals, HPLC grade) and then added to the

ACPD
13, 14613–14635, 2013

chamber by injecting the appropriate volume of liquid into a stream of purified air. The injection port, the short inlet line (10 cm) and the air were heated to 60 °C to minimize the losses during the injection.

The gas phase concentration in the chamber was monitored using a high-resolution proton transfer reaction mass spectrometer (PTR-TOF-MS 8000, Ionicon Analytik, Innsbruck, Austria). Sample air from the chamber was introduced to the PTR drift tube via a 1.5 m long heated (60 °C) PEEK tubing (outer diameter 1/16 inches) at a flow rate of 160 mL min^{-1}. PTR-TOF-MS was operated under controlled conditions (2.3 mbar drift tube pressure, 600 V drift tube voltage and 60 °C temperature). The sensitivity of PTR-TOF for the studied compounds was calibrated using the gas phase concentration results from Tenax TA samples. Within 30 min after the injection the gas phase concentration in the chamber had stabilized and VOC samples were collected onto 200 mg of Tenax TA adsorbent (Supelco, mesh 60/80) for 10 to 30 min with an air flow of 220 mL min^{-1} through the sample tube. The sampling time depended on the injected concentration so that for the lowest concentration the sampling time was longest to obtain high enough amount of VOC for the analysis. Tenax TA adsorbent was connected directly to the chamber without any sample line to reduce wall losses during sampling. The trapped compounds were desorbed from the collected VOC samples with a thermal desorption unit (Perkin-Elmer ATD400 Automatic Thermal Desorption system) and analyzed with a gas chromatograph-mass spectrometer (Hewlett-Packard GC 6890 and MSD 5973). A detailed description of the VOC analysis can be found in (Vuorinen et al., 2004). In order to avoid significant formation of particles, the concentrations of the injected compounds were kept small. To affirm low new particle formation, the particle concentrations were continuously followed by a condensation particle counter (CPC3010, TSI).

2.2 SOA formation experiment

The dynamics of organic aerosol formation, and in particular, the implications of measured wall losses of SOA precursors were studied in an α-pinene ozonolysis experi-

ACPD
13, 14613–14635, 2013

ment in the presence of seed aerosol. As the seed aerosol, we used polydisperse ammonium sulphate particles which were generated from a salt-solution using an aerosol generator (Model 3076, TSI Inc., USA). The ammonium sulphate content in the water suspension was 1 wt-%. The produced aerosol was fed to a diffusion drier (porous tube surrounded by silica gel), resulting in a relative humidity (RH) of below 5 % (RH sensor, Rotronic).

After introducing the seed aerosol to the flushed Teflon chamber, its concentration was diluted to ($\sim 10^4\,cm^{-3}$). Next, 2 µL of α-pinene was injected to the chamber and left to mix for 15 min. In the next step of the experiment, ozone enriched air (1.5 ppm, generated with a UV lamp O_3 generator) was introduced into the chamber at 30 L min^{-1} to achieve an ozone concentration of 50 ppb. The ozonolysis of α-pinene resulted in a clear nucleation and growth event which was monitored with two scanning mobility particle sizers (SMPS: SMPS1: CPC3027 & DMA 3075; SMPS2: CPC 3022 & DMA 3071) with measurement ranges from 3–60 nm and 10–700 nm. The temperature during the experiment was 25 ± 2 °C and RH 5 ± 2 %.

Real-time chemical composition in the particles with vacuum aerodynamic diameter size ranging from 50 to 1000 nm was measured using Aerodyne HR-TOF-AMS (High Resolution Time-Of-Flight Aerosol Mass Spectrometer) (Jayne et al., 2000; DeCarlo et al., 2006) using standard 600 °C vaporizer temperature. Sulphate, organics, ammonium and nitrate mass loadings were determined in high resolution and O/C ratios by elemental analysis in HR analysis panel in Igor pro.

The evolution of the aerosol size distribution during a SOA formation experiment was simulated using the sectional aerosol model SALSA (Kokkola et al., 2008), which was modified by including a SOA chemistry module which uses the VBS approach. The gas phase kinetics was calculated using an ordinary differential equation solver (Radhakrishnan and Hindmarsh, 1993).

A detailed description of the methods used to solve the aerosol microphysical processes in the model is given by Kokkola et al. (2008). The aerosol particle wall losses in the model were determined by seeding the chamber with a known population of am-

ACPD
13, 14613–14635, 2013

monium sulfate particles in the absence of condensing vapors and measuring the time evolution of the size distribution. A functional form of the wall loss rates was obtained by minimizing the difference between the measured and modeled size distributions.

When simulating SOA formation in the chamber, the background size distribution was initialized using the measured number size distribution from SMPS. Furthermore, nucleation was not explicitly modeled but the number concentrations measured in the two smallest size channels of SMPS were read into the model throughout a simulation.

3 Results and discussion

3.1 Gas–wall equilibrium partitioning

The gas–wall equilibrium as a function of saturation vapor pressure of OVOC's was determined by injecting three organic gases of different volatilities in a Teflon chamber while measuring which fraction of the total amount of injected compound remains in the gas phase. In this experiment, a constant amount of α-pinene, nopinone, and pinanediol were injected into the chamber in 30 min intervals for the duration of several hours. The motivation for such experiment was to evaluate if and on which scale a steady-state equilibrium between the walls and the gas is reached. This way we were also able to determine if the fractions of compounds partitioned on the chamber walls were independent of total amounts of the compounds in the chamber or if the walls were saturated at some point thus affecting the equilibrium between the walls and the gas.

Figure 2a illustrates the observed evolution of gas phase concentration during the experiment. An equilibrium concentration for all three measured compounds was reached within minutes after each injection after which the concentration remained approximately constant. This clearly demonstrates that the chamber walls do not act as a continuous sink for the injected compounds.

ACPD
13, 14613–14635, 2013

As the deposition of the compounds to the chamber walls is a dynamical process, deposition of each organic compound OC was assumed to follow the equation

$$\frac{\mathrm{d}[\mathrm{OC}]_\mathrm{w}}{\mathrm{d}t} = k\left[\left(\frac{K_\mathrm{p}}{(K_\mathrm{p}+1)}\right)[\mathrm{OC}]_\mathrm{T} - [\mathrm{OC}]_\mathrm{w}\right] \quad (3)$$

where k (s^{-1}) is the mass transfer coefficient, i.e. a parameter that dictates the characteristic time for reaching the equilibrium between the walls and the chamber.

We estimated the equilibration time by solving analytically the wall concentration $[\mathrm{OC}]_\mathrm{w}$ from Eq. (3) and then optimizing the mass transfer coefficient k so that evolution of $[\mathrm{OC}]_\mathrm{w}$ as a function of time matched the measured evolution of $[\mathrm{OC}]_\mathrm{w}$ for each injection. The mass transfer coefficient was optimized using an unconstrained nonlinear optimization method (Nelder and Mead, 1965). However, due to significant noise in the PTR-MS-TOF measured concentrations, the fitted values for k ranged greatly between the injections and our measurements were able to provide only a qualitative estimate of the mass transfer rate. For nopinone, the fitted k values ranged from 0.03 to 0.79. For pinanediol, there was no distinct peak in the gas phase concentration during the injection; instead the concentration slowly increased to its new equilibrium value. Because of this, the mass transfer coefficient could not be determined. However, within the scope of this study, we were not able to identify the mechanisms causing this behavior.

We also tested if the simultaneous injection of these compounds would affect their equilibrium concentrations by injecting the gases sequentially into the chamber. Measurements did not show any change in the equilibrium concentration of the gas which was injected first after a second gas was injected.

Figure 2b shows the fractions of α-pinene, nopinone, and pinanediol that were deposited on the chamber walls after each injection as a function of saturation concentration of the compounds. The mean fractions were 0.40 and 0.82 for nopinone and pinanediol, respectively. α-pinene remained completely in the gas phase. The noise in the data resulted in fairly large uncertainty and translated to variability in the estimated

ACPD
13, 14613–14635, 2013

wall-fractions of each compound. Especially, since the measured gas phase concentrations of pinanediol were low with respect to the variability in the measurements, the estimated wall-fractions also show large variability in Fig. 2b. However, there was no correlation between the wall-fraction and the total concentration of any of the compounds, indicating that the Henry's law type equilibrium assumption holds for these concentrations and that the chamber walls were not saturated with respect to the depositing gases at any point of the experiment.

Based on these measured values and Eqs. (1) and (2), we calculated the theoretical fraction of OC on the chamber walls as a function of saturation concentration which is a measure of the OVOC volatility. Equation (1) requires knowledge about the effective concentration of OC on the chamber walls (C_w), which is dependent on the properties of each compound (Matsunaga and Ziemann, 2010). We assumed C_w to be equal for all oxidation products of α-pinene and set it to 1.1×10^3 mg m^{-3}, which is the average value for nopinone and pinanediol in our wall loss experiments. Using this value, we can calculate the theoretical fraction of OC partitioning to the walls as a function of saturation concentration (solid blue curve in Fig. 2b). The dotted vertical lines in Fig. 2b show the saturation concentrations for typically used volatility classes in VBS (Pathak et al., 2007). Although, the wall fractions of individual compounds do not fall exactly on the theoretical curve, we use this as a first-order approximation for equilibrium partitioning later in our aerosol microphysics modeling. Based on this theoretical curve we can see that for all the VBS volatility classes, practically all OC should be on the chamber walls once equilibrium between the gas-phase and the walls is formed.

As can be seen from Fig. 2b, the compounds used in our study have higher volatility than commonly used VBS volatility classes. This is because our method of measuring gaseous wall losses requires that there is no new particle formation from low volatile compounds during an experiment. For the organic gases used in this study, we did not observe a significant number of particles during the measurement. However, we carried out a similar experiment as described above also for cis-pinonic acid which has a saturation concentration of the order of 10^3 µm^{-3} (Jimenez et al., 2009); i.e. an order

ACPD
13, 14613–14635, 2013

of magnitude lower than that of pinanediol. In this experiment there was significant formation of new particles which prevented the estimation of the OVOC's equilibrium wall losses. Therefore, using the method presented in this study, we are unable to determine experimentally the wall losses for the commonly used VBS classes. To verify that the theoretical curve in Fig. 2b applies also for the whole range of volatilities, new methods for measuring the wall fraction of low volatility organic gases would be needed.

3.2 SOA formation experiment

Next, we applied the volatility dependent wall loss function Eq. (3) to the aerosol microphysics model to investigate the implications of gas-phase wall losses in a SOA formation chamber experiment. In this experiment ammonium sulfate seed aerosol was fed into the chamber followed by an injection of α-pinene and ozone. Figure 3a illustrates the measured evolution of the aerosol size distribution during the experiment. We can see that after the injection of α-pinene and ozone, a new particle formation event occurs and a distinct nucleation mode appears in the size distribution. Since the nucleation mode particles grow to 10 nm within few minutes of the injection of ozone, it is evident that a significant amount of LVOC's capable of growing nanometer sized particles form in the chamber during the first steps of alpha-pinene oxidation. The composition of larger (> 80 nm) particles was measured using an aerosol mass spectrometer (AMS) throughout the experiment.

According to the measurements, when the nucleation mode appears in the size distribution, organic mass fraction in the seed aerosol rapidly increased to about 0.3 supporting the conclusion that the new particles were grown by LVOC's. From the AMS data, we were also able to estimate the volatility of the condensed matter. The oxygen to carbon atomic ratio (O : C) of the particles has been shown to correlate with the volatility of the aerosol and therefore be used to estimate if the aerosol consists LVOC or semi-volatile organic compounds (SVOC) (Jimenez et al., 2009). During the formation of the nucleation mode, the average O : C ratio reached 0.4 within one hour from the injection of ozone after which the ratio stayed approximately at a constant

ACPD
13, 14613–14635, 2013

level. According to previous studies (Jimenez et al., 2009), such O : C ratio indicates that the condensed organics are of low volatility. As this is the mean O : C of the total sampled aerosol mass, there is a possibility that a fraction of condensing matter is of very low volatility. The fingerprint for the presence of LVOC's of extra low volatility is the formation and growth of the nanometer sized particles as we will show below.

3.3 Modeling the SOA formation experiment

To evaluate the role of wall losses and the contribution of OVOC's of different volatilities to the evolution of aerosol size distribution, this SOA formation experiment was simulated using the aerosol microphysics code SALSA (Kokkola et al., 2008). We assumed stoichiometric coefficients given in Table 1 (Pathak et al., 2007) for the commonly used VBS volatility classes (vertical dashed lines in Fig. 3b) in modeling oxidation of α-pinene by ozone. Based on the wall loss experiments, we assumed that the mass transfer coefficient to the walls is $0.03\,s^{-1}$ for all volatility classes which is the lower limit of estimated values from the wall-loss experiment described in the previous section.

Figure 3b shows the modeled evolution of the aerosol size distribution. Clearly, the stoichiometric coefficients typically used for VBS do not produce enough low-volatility gases to reproduce the growth of the nucleation mode particles. To reproduce the growth, we optimized the value for the stoichiometric coefficients of the volatility class of the lowest volatility class using an unconstrained nonlinear optimization method (Nelder and Mead, 1965) so that the difference between the observed and modeled total number concentrations in sizes below 40 nm in diameter were minimized. The optimization resulted in significantly higher stoichiometric coefficient for the lowest volatility class; our optimized value was 0.14, which is approximately two orders of magnitude higher than the original value of 0.001. When we used the optimized values, the model was able to simulate the new particle event as can be seen from Fig. 3c. According to our model calculations, the increase in the stoichiometric coeffient resulted in a 4 times larger mass yield for the SOA of lowest volatility. However, when we used the op-

ACPD
13, 14613–14635, 2013

timized stoichiometric coefficient there was noticeable evaporation of SOA at approximately 2.5 h into the simulation, which was not seen in the measured size distribution. To overcome this discrepancy, we added the volatility of the lowest VBS class as an optimization parameter and repeated the optimization. When we optimized the volatility and the stoichiometric coefficient concurrently, the best fit was obtained when the equilibrium concentration was $2.5 \times 10^{-5}\,\mu g\,m^{-3}$ and the stoichiometric coefficient was 0.1. We can see from Fig. 3d that when using these values, the agreement between the measured and modeled size distribution increased even further as there was no evaporation of the simulated nucleation mode particles. This also indicates that there is a significant amount of LVOC's formed in the chamber.

These compounds of low volatility would be difficult to observe in chamber measurements because of two factors. First, according to our model simulation in which the volatility of the OVOC of the lowest volatility was assumed to be $2.5 \times 10^{-5}\,\mu g\,m^{-3}$, approximately 60 % of its total amount was deposited on the chamber walls already when the new particle formation was detected. By the end of the experiment, approximately 95 % of it was deposited on the chamber walls. In addition, according to our model and the AMS data, in a type of an experiment that was presented in this study, the organic fraction dominates the aerosol mass only in sizes smaller than 80 nm in diameter, making it also difficult to collect a large enough sample to properly measure the low volatile condensed matter. During chamber experiments, these would cause significant difficulties in collecting large enough samples for the measurement devices to detect the very low volatility compounds. In ambient conditions, the fraction that would be lost on the walls during chambers experiments would amount to a significant fraction in the aerosol mass as there would not be a similar competing process for the condensing OVOC's in the atmosphere. This additional condensing matter would significantly affect the number particles that can act as cloud condensation nuclei (CCN).

It should be noted that our model describes the gas phase chemistry and aerosol processes in a simplified manner and can only qualitatively simulate aerosol growth process. There can also be other mechanism that would explain the fact that evapo-

ACPD
13, 14613–14635, 2013

ration of the nucleation mode is not seen in the measurements. For example, particle phase diffusion and chemical transformation are not included in the model which could potentially have significant effects on evolution of the aerosol size distribution. It has been also suggested that SOA particles are solid (Virtanen et al., 2010) which would reduce evaporation rate due to the diffusional limitations of molecules in the particle bulk (Cappa and Jimenez, 2010; Vaden et al., 2010; Abramson et al., 2013).

4 Conclusions

We have analyzed a new particle formation event in a chamber to probe the role of organic vapors in new particle formation and their gas particle partitioning. By comparing the observed rates of wall deposition and initial particle growth to a detailed aerosol dynamics simulation, we arrived at the following main conclusions:

1. To comprehensively determine the aerosol mass yields for OVOC of different volatilies in Teflon chamber studies, the wall losses of gas phase OVOC should be carefully accounted for taking into account their volatility. Because of the rapid depletion of OVOC of lowest volatilities to the chamber walls, their yields can be significantly underestimated. In our simulation on chamber experiment where SOA was formed on pre-existing ammonium sulfate aerosol, we estimated that the aerosol mass yield can be underestimated by a factor of four.

2. Organic vapor(s) with very low volatility are formed directly as reaction products of our injected α-pinene and ozone. These vapors are responsible for a significant fraction of the observed early growth, but deposit and reach equilibrium with the walls very quickly resulting in stoppage of growth. According to our model simulations the observed nucleation mode in the presence of dominant loss of condensing organics on the walls necessitates the inclusion of significant amount of organics of very low volatility. Optimizing model agreement with measurements suggests volatilities of the order of $1 \times 10^{-5}\,\mu g\,m^{-3}$. The current understanding of

ACPD
13, 14613–14635, 2013

the formation of organic vapors with such low volatilities suggests a rather long chain of oxidation reactions contradicting the observations of our study.

3. At ambient conditions, the key implication of our study is increased mass yield from low volatile compounds that can contribute significantly to the number concentration of nucleated particles which grow to sizes that can take part in cloud activation. At the same time, the majority of these LVOC's condense on the condensation sink, contributing to the growth and evolution of the entire aerosol distribution.

Acknowledgements. This work was supported by the Maj and Tor Nessling Foundation (Project nr. 2012358), the Academy of Finland (projects nr. 252908 and 138951), the Academy of Finland Centre of Excellence Program (project nr 1118615), and the strategic funding of the University of Eastern Finland.

References

Abramson, E., Imre, D., Beránek, J., Wilson, J., and Zelenyuk, A.: Experimental determination of chemical diffusion within secondary organic aerosol particles, Phys. Chem. Chem. Phys., 15, 2983–2991, 2013. 14627

Cappa, C. D. and Jimenez, J. L.: Quantitative estimates of the volatility of ambient organic aerosol, Atmos. Chem. Phys., 10, 5409–5424, doi:10.5194/acp-10-5409-2010, 2010. 14627

Ceulemans, K., Compernolle, S., and Müller, J.-F.: Parameterising secondary organic aerosol from α-pinene using a detailed oxidation and aerosol formation model, Atmos. Chem. Phys., 12, 5343–5366, doi:10.5194/acp-12-5343-2012, 2012. 14615

DeCarlo, P. F., Kimmel, J. R., Trimborn, A., Northway, M. J., Jayne, J. T., Aiken, A. C., Gonin, M., Fuhrer, K., Horvath, T., Docherty, K. S., Worsnop, D. R., and Jimenez, J. L.: Field-deployable, high-resolution, time-of-flight aerosol mass spectrometer, Anal. Chem., 78, 8281–8289, doi:10.1021/ac061249n, 2006. 14620

Donahue, N. M., Robinson, A. L., Stanier, C. O., and Pandis, S. N.: Coupled partitioning, dilution, and chemical aging of semivolatile organics, Env. Sci. Tech., 40, 2635–2643, doi:10.1021/es052297c, 2006. 14616

Duplissy, J., DeCarlo, P. F., Dommen, J., Alfarra, M. R., Metzger, A., Barmpadimos, I., Prevot, A. S. H., Weingartner, E., Tritscher, T., Gysel, M., Aiken, A. C., Jimenez, J. L., Canagaratna, M. R., Worsnop, D. R., Collins, D. R., Tomlinson, J., and Baltensperger, U.: Relating hygroscopicity and composition of organic aerosol particulate matter, Atmos. Chem. Phys., 11, 1155–1165, doi:10.5194/acp-11-1155-2011, 2011. 14616

Goldstein, A. H. and Galbally, I. E.: Known and unexplored organic constituents in the Earth's atmosphere, Env. Sci. Tech., 41, 1514–1521, doi:10.1021/es072476p, 2007. 14615

Hallquist, M., Wenger, J. C., Baltensperger, U., Rudich, Y., Simpson, D., Claeys, M., Dommen, J., Donahue, N. M., George, C., Goldstein, A. H., Hamilton, J. F., Herrmann, H., Hoffmann, T., Iinuma, Y., Jang, M., Jenkin, M. E., Jimenez, J. L., Kiendler-Scharr, A., Maenhaut, W., McFiggans, G., Mentel, Th. F., Monod, A., Prévôt, A. S. H., Seinfeld, J. H., Surratt, J. D., Szmigielski, R., and Wildt, J.: The formation, properties and impact of secondary organic aerosol: current and emerging issues, Atmos. Chem. Phys., 9, 5155–5236, doi:10.5194/acp-9-5155-2009, 2009. 14615

Hao, L. Q., Romakkaniemi, S., Yli-Pirilä, P., Joutsensaari, J., Kortelainen, A., Kroll, J. H., Miettinen, P., Vaattovaara, P., Tiitta, P., Jaatinen, A., Kajos, M. K., Holopainen, J. K., Heijari, J., Rinne, J., Kulmala, M., Worsnop, D. R., Smith, J. N., and Laaksonen, A.: Mass yields of secondary organic aerosols from the oxidation of α-pinene and real plant emissions, Atmos. Chem. Phys., 11, 1367–1378, doi:10.5194/acp-11-1367-2011, 2011. 14618

Jayne, J. T., Leard, D. C., Zhang, X., Davidovits, P., Smith, K. A., Kolb, C. E., and Worsnop, D. R.: Development of an aerosol mass spectrometer for size and composition analysis of submicron particles, Aerosol Sci. Tech., 33, 49–70, http://www.ingentaconnect.com/content/tandf/uast/2000/00000033/F0020001/art00005, 2000. 14620

Jimenez, J. L., Canagaratna, M. R., Donahue, N. M., Prevot, A. S. H., Zhang, Q., Kroll, J. H., DeCarlo, P. F., Allan, J. D., Coe, H., Ng, N. L., Aiken, A. C., Docherty, K. S., Ulbrich, I. M., Grieshop, A. P., Robinson, A. L., Duplissy, J., Smith, J. D., Wilson, K. R., Lanz, V. A., Hueglin, C., Sun, Y. L., Tian, J., Laaksonen, A., Raatikainen, T., Rautiainen, J., Vaattovaara, P., Ehn, M., Kulmala, M., Tomlinson, J. M., Collins, D. R., Cubison, M. J. E., Dunlea, J., Huffman, J. A., Onasch, T. B., Alfarra, M. R., Williams, P. I., Bower, K., Kondo, Y., Schneider, J., Drewnick, F., Borrmann, S., Weimer, S., Demerjian, K., Salcedo, D., Cottrell, L., Griffin, R., Takami, A., Miyoshi, T., Hatakeyama, S., Shimono, A., Sun, J. Y., Zhang, Y. M., Dzepina, K., Kimmel, J. R., Sueper, D., Jayne, J. T., Herndon, S. C., Trimborn, A. M., Williams, L. R., Wood, E. C., Middlebrook, A. M., Kolb, C. E., Baltensperger, U.,

ACPD
13, 14613–14635, 2013

and Worsnop, D. R.: Evolution of organic aerosols in the atmosphere, Science, 326, 1525–1529, doi:10.1126/science.1180353, 2009. 14614, 14615, 14623, 14624, 14625

Kokkola, H., Korhonen, H., Lehtinen, K. E. J., Makkonen, R., Asmi, A., Järvenoja, S., Anttila, T., Partanen, A.-I., Kulmala, M., Järvinen, H., Laaksonen, A., and Kerminen, V.-M.: SALSA – a Sectional Aerosol module for Large Scale Applications, Atmos. Chem. Phys., 8, 2469–2483, doi:10.5194/acp-8-2469-2008, 2008. 14620, 14625

Kroll, J. H. and Seinfeld, J. H.: Chemistry of secondary organic aerosol: formation and evolution of low-volatility organics in the atmosphere, Atmos. Environ., 42, 3593–3624, doi:10.1016/j.atmosenv.2008.01.003, 2008. 14615

Matsunaga, A. and Ziemann, P. J.: Gas–wall partitioning of organic compounds in a teflon film chamber and potential effects on reaction product and aerosol yield measurements, Aerosol Sci. Tech., 44, 881–892, doi:10.1080/02786826.2010.501044, 2010. 14616, 14623

Meyer, N. K., Duplissy, J., Gysel, M., Metzger, A., Dommen, J., Weingartner, E., Alfarra, M. R., Prevot, A. S. H., Fletcher, C., Good, N., McFiggans, G., Jonsson, Å. M., Hallquist, M., Baltensperger, U., and Ristovski, Z. D.: Analysis of the hygroscopic and volatile properties of ammonium sulphate seeded and unseeded SOA particles, Atmos. Chem. Phys., 9, 721–732, doi:10.5194/acp-9-721-2009, 2009. 14616

Nelder, J. A. and Mead, R.: A simplex method for function minimization, Comput. J., 7, 308–313, doi:10.1093/comjnl/7.4.308, 1965. 14622, 14625

Odum, J. R., Hoffmann, T., Bowman, F., Collins, D., Flagan, R. C., and Seinfeld, J. H.: Gas/particle partitioning and secondary organic aerosol yields, Env. Sci. Tech., 30, 2580–2585, doi:10.1021/es950943+, 1996. 14616

Pathak, R. K., Presto, A. A., Lane, T. E., Stanier, C. O., Donahue, N. M., and Pandis, S. N.: Ozonolysis of α-pinene: parameterization of secondary organic aerosol mass fraction, Atmos. Chem. Phys., 7, 3811–3821, doi:10.5194/acp-7-3811-2007, 2007. 14616, 14623, 14625

Pierce, J. R., Engelhart, G. J., Hildebrandt, L., Weitkamp, E. A., Pathak, R. K., Donahue, N. M., Robinson, A. L., Adams, P. J., and Pandis, S. N.: Constraining particle evolution from wall losses, coagulation, and condensation-evaporation in smog-chamber experiments: optimal estimation based on size distribution measurements, Aerosol Sci. Tech., 42, 1001–1015, doi:10.1080/02786820802389251, 2008. 14616

ACPD
13, 14613–14635, 2013

Radhakrishnan, K. and Hindmarsh, A. C.: Description and use of LSODE, the Livermore Solver for Ordinary Differential Equations, LLNL Report UCRL-ID-113855, Lawrence Livermore National Laboratory, Livermore, California, 1993. 14620

Riipinen, I., Pierce, J. R., Yli-Juuti, T., Nieminen, T., Häkkinen, S., Ehn, M., Junninen, H., Lehtipalo, K., Petäjä, T., Slowik, J., Chang, R., Shantz, N. C., Abbatt, J., Leaitch, W. R., Kerminen, V.-M., Worsnop, D. R., Pandis, S. N., Donahue, N. M., and Kulmala, M.: Organic condensation: a vital link connecting aerosol formation to cloud condensation nuclei (CCN) concentrations, Atmos. Chem. Phys., 11, 3865–3878, doi:10.5194/acp-11-3865-2011, 2011. 14615

Vaden, T. D., Song, C., Zaveri, R. A., Imre, D., and Zelenyuk, A.: Morphology of mixed primary and secondary organic particles and the adsorption of spectator organic gases during aerosol formation, P. Natl. Acad. Sci. USA, 107, 6658–6663, 2010. 14627

Virtanen, A., Joutsensaari, J., Koop, T., Kannosto, J., Yli-Pirila, P., Leskinen, J., Makela, J. M., Holopainen, J. K., Poschl, U., Kulmala, M., Worsnop, D. R., and Laaksonen, A.: An amorphous solid state of biogenic secondary organic aerosol particles, Nature, 467, 824–827, doi:10.1038/nature09455, 2010. 14627

Vuorinen, T., Nerg, A.-M., Ibrahim, M. A., Reddy, G. V. P., and Holopainen, J. K.: Emission of *Plutella xylostella*-induced compounds from cabbages grown at elevated CO_2 and orientation behavior of the natural enemies, Plant Physiol., 135, 1984–1992, doi:10.1104/pp.104.047084, 2004. 14619

Zhao, J., Ortega, J., Chen, M., McMurry, P. H., and Smith, J. N.: Dependence of particle nucleation and growth on high molecular weight gas phase products during ozonolysis of α-pinene, Atmos. Chem. Phys. Discuss., 13, 9319–9354, doi:10.5194/acpd-13-9319-2013, 2013. 14615

ACPD
13, 14613–14635, 2013

Table 1. Saturation concentrations C^* ($\mu g\,m^{-3}$) and corresponding stoichiometric coefficients α for VBS classes.

C^*	0.01	0.1	1.0	10	100	1000	10 000
α	0.001	0.012	0.037	0.088	0.099	0.250	0.80

ACPD
13, 14613–14635, 2013

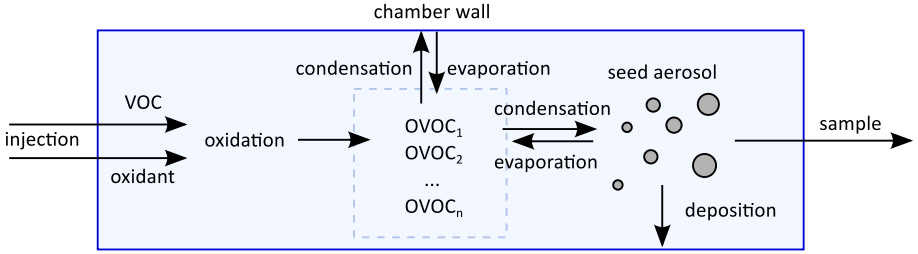

Fig. 1. Schematic of processes modifying the concentrations of particle and gas phase OVOC's during a oxidation chamber experiment.

ACPD
13, 14613–14635, 2013

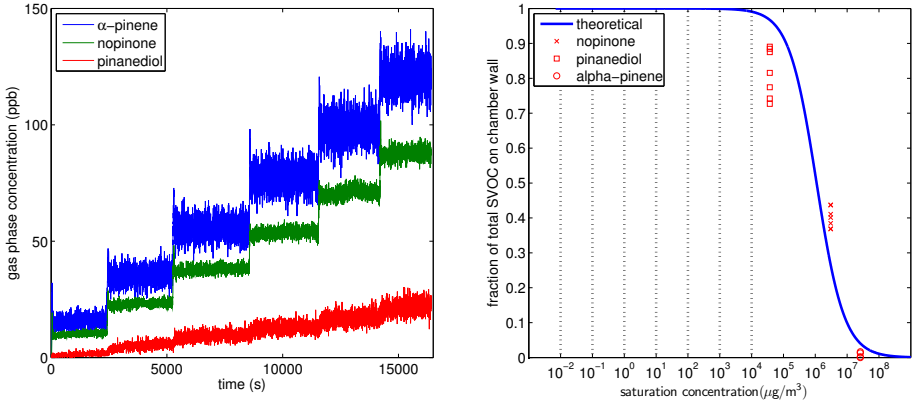

Fig. 2. **(a)** Time dependent gas phase concentration of α-pinene, nopinone, and pinanediol. **(b)** Measured fractions of the same three compounds on chamber walls (red symbols) and a theoretical extrapolation of the measurements to other volatilities (blue line). The vertical dotted lines indicate the commonly assumed VBS volatility bins.

ACPD
13, 14613–14635, 2013

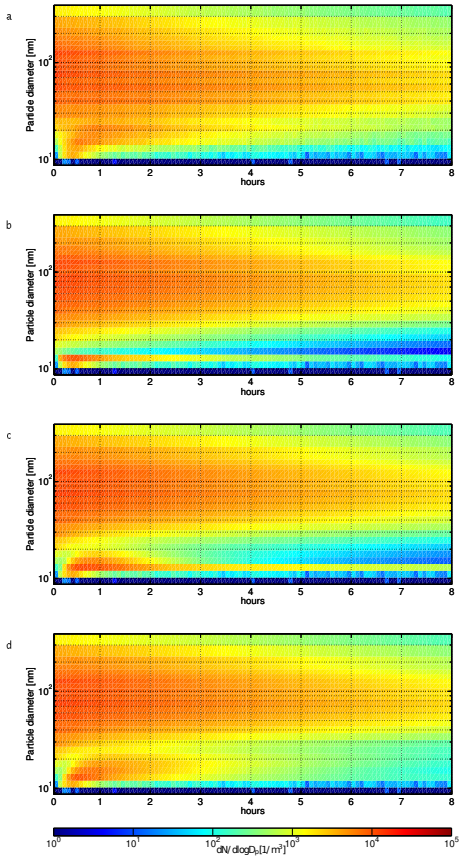

Fig. 3. (a) Observed evolution of aerosol size distribution, **(b)** modeled evolution of aerosol size distribution using stoichiometric coefficients given in Table 1 **(c)** modeled evolution of aerosol size distribution using optimized stoichiometric coefficient for the lowest volatility class **(d)** modeled evolution of aerosol size distribution using optimized volatility and stoichiometric coefficient for the lowest volatility class.

ACPD
13, 14613–14635, 2013